

## Quantum Chemical Investigations on Electron Transport Characteristics of Porphyrin and Metal-porphyrin \*

OUYANG Sheng-de<sup>1</sup>, YI Yuan-ping<sup>1</sup>, GENG Hua<sup>1</sup>, SHUAI Zhi-gang<sup>1\*\*</sup> and LUO Yi<sup>2\*\*</sup>

1. *Key Laboratory of Organic Solids, Institute of Chemistry, Chinese Academy of Sciences, Beijing 100080, P. R. China;*

2. *Theoretical Chemistry, Royal Institute of Technology, AlbaNova, Stockholm S-106 91, Sweden*

Received Mar. 20, 2006

Recently, molecular electronics has become increasingly important. By applying the hybrid density functional theory coupled with the Green's function method, the current-voltage characteristics of the molecular junctions composed of gold-porphyrin-gold and gold-copper porphyrin-gold were investigated. The role of the metal coordination effect in organic molecular electron transport was highlighted. Although the thresholds of the bias voltage for both molecules were almost the same, approximately 0.9 V, the metal compound showed a larger increase in current because of the metal-coordination-enhanced molecule-electrode coupling in the frontier molecular orbitals.

**Keywords** Electron transport; Elastic-scattering; Transmission

### Introduction

Recently, great advances have been made in the research of molecular electronics<sup>[1,2]</sup>. Molecular devices based on single molecule<sup>[3–5]</sup> or molecular clusters<sup>[6–8]</sup>, negative differential resistance<sup>[9]</sup>, electrostatic current switching<sup>[10–12]</sup>, atomic wires<sup>[13]</sup>, short organic molecule wires<sup>[3,14,15]</sup>, long-chain polymers<sup>[16]</sup>, carbon nanotube<sup>[17]</sup>, and fullerene<sup>[18]</sup> have been reported. Despite the recent advances, it is still very difficult to control the device fabrication, and the measurement is far from consolidated. Therefore, reliable computational approaches on the molecular junctions are necessary.

The quantum theory has been extremely successful in describing the electron transports in solids. These approaches have been adopted in molecular electronics<sup>[19–25]</sup>. Ratner and colleagues<sup>[19]</sup> have extended the application scope of elastic scattering Green's function theory to studying the electron transport. Based on the first-principle density functional theory, various approaches have been developed to study the parameters of molecular electronics. Lang and coworkers<sup>[26,27]</sup> developed DFT-plane wave basis plus Lippman-Schwinger scattering equation formalism, where the electrode was

treated as the jellium model. Guo *et al.*<sup>[28,29]</sup> developed a real-space DFT coupled with Keldysh nonequilibrium Green's function formalism, which treats the electrode and the molecule on equal footings. Yang *et al.*<sup>[30]</sup> developed a similar approach that allows for calculating complex molecular systems.

Despite the great theoretical advances, there still exists a discrepancy between the measurement and the computation. For instance, the current value at fixed bias is calculated to be two orders of magnitude greater than the measurement for the simplest molecule dithiol-benzene. On the one hand, it is very difficult to manipulate the molecular device fabrication, especially, the details of the contact between the molecule and the electrode, and the surface morphologies of the solid can strongly influence the  $I-V$  characteristics. On the other hand, so far the theoretical methodology has been based on approximating the Kohn-Sham orbital as the real single particle without considering the electron correlation effects. In fact, a recent study based on molecular electron-correlated excited states has indicated that the electron correlation effect plays an important role in determining the molecular electron transport behavior. Geng *et al.*<sup>[31]</sup> found that the molecule-elec-

\* Supported by the National Natural Science Foundation of China (Nos. 90301001 and 10425420) and the Supercomputing Center of the Chinese Academy of Sciences.

\*\* To whom corresponding should be addressed. E-mail: zgshuai@iccas.ac.cn; luo@theochem.kth.seIntroduction

trode contact largely influences the electric current, and the intermolecular interaction can cause tunneling through intermolecular charge transfer. Most interestingly, Luo and colleagues<sup>[24,25]</sup>, and Wang *et al.*<sup>[32]</sup> revealed that the theoretical consideration of the dimensionality of the electrode plays a key role in the calculation of the current-voltage characteristics through the density of states near the electrode Fermi surface, which can considerably improve the previous results obtained by Ratner *et al.*<sup>[19]</sup> and Datta *et al.*<sup>[20]</sup> within the equilibrium Green's function approach.

In this study, the methodology of this approach is briefly described and is applied for investigating the electron transport in porphyrin and Cu-porphyrin, to reveal the role of metal-organic ligand interaction in molecular electronic devices.

### Theoretical Methodology

The typical molecular device consists of metal (source)-molecule-metal (drain) junctions (see Fig. 1). The electrode is modeled as three Au atoms, as in the previous cases<sup>[24,25,32]</sup>. In fact, it has been shown that the discreteness of the molecular orbital levels do not affect the results to a large extent because it is the Fermi level, taken as the midlevel of HOMO and LUMO, which is not sensitive to the cluster size. The extended system is shown in Fig. 1.

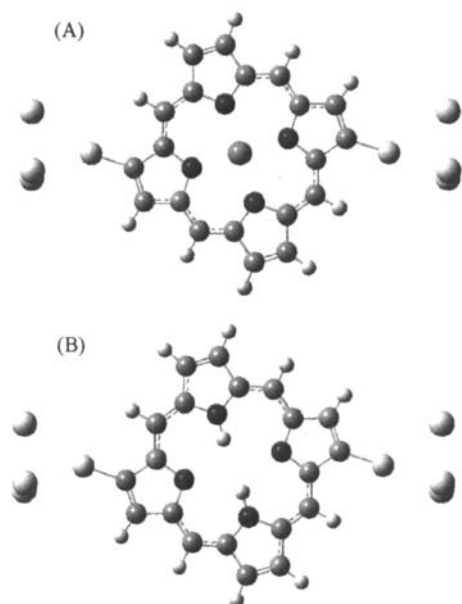


Fig. 1 Molecular device for Au-CuPorphyrin-Au (A) and Au-Porphyrin-Au (B)

The molecular orbitals satisfy the following equation:

$$H|\Psi_{\eta}\rangle = \varepsilon_{\eta}|\Psi_{\eta}\rangle \quad (1)$$

where the Hamiltonian of the system has the following matrix structure:

$$H = \begin{vmatrix} H^{SS} & H^{SM} & H^{SD} \\ H^{MS} & H^{MM} & H^{MD} \\ H^{DS} & H^{DM} & H^{DD} \end{vmatrix}$$

where  $H^{SS}$ ,  $H^{MM}$ , and  $H^{DD}$  are the matrices for the subsystems of source, drain, and molecules, respectively.

Based on the elastic scattering Green's function theory<sup>[33,34]</sup>, the transmission operator is defined as:

$$T = U + UG^0T = U + UGU \quad (2)$$

Here,

$$G^0(z) = (z - H_0)^{-1}, G(z) = (z - H)^{-1} \quad (3)$$

The transition element from the initial source state  $|l\rangle$  elastically scattered to the final drain state  $|l'\rangle$  is:

$$T_{l'l} = \langle l' | T | l \rangle = \langle l' | U | l \rangle + \langle l' | UGU | l \rangle \quad (4)$$

The direct coupling between the source and the drain can be neglected,  $\langle l' | U | l \rangle = 0$ . Thus the following equation is obtained:

$$\begin{aligned} T_{l'l} &= \langle l' | UGU | l \rangle \\ &= \sum_{\tilde{j}} \langle l' | U | i \rangle \langle i | \frac{1}{z - H} | j \rangle \langle j | U | l \rangle \\ &= \sum_{\eta} \sum_{\tilde{j}} \langle l' | U | i \rangle \langle i | \frac{1}{z - H} | \eta \rangle \langle \eta | j \rangle \\ &\quad \langle j | U | l \rangle \end{aligned} \quad (5)$$

Note that

$$\begin{aligned} G_{\tilde{j}} &= \sum_{\eta} \langle i | \frac{1}{z - H} | \eta \rangle \langle \eta | j \rangle \\ &= \sum_{\eta} \frac{\langle i | \eta \rangle \langle \eta | j \rangle}{z - \varepsilon_{\eta}} \end{aligned} \quad (6)$$

and

$$T_{l'l} = \sum_{\tilde{j}} \langle l' | U | i \rangle G_{\tilde{j}} \langle j | U | l \rangle \quad (7)$$

Here, the argument in the Green's function  $G_{\tilde{j}}$  is a complex number,  $z = E + i\Gamma_{\eta}$ ,  $E$  is the elastic scattering energy of electrons, and  $\Gamma_{\eta}$  is a broadening factor for level  $\eta$  attributed to the molecule-electrode coupling.

By combining all the initial and final states in the scattering process, the following equation is obtained:

$$T = \sum_{\tilde{j}} \sum_{\eta} \sum_{l'l} \frac{\langle l' | U | i \rangle \langle i | \eta \rangle \langle \eta | j \rangle \langle j | U | l \rangle}{z - \varepsilon_{\eta}} \quad (8)$$

Denoting that

$$N_{\eta} = \sum_{l'i} \langle l' | U | i \rangle \langle i | \eta \rangle \quad (9)$$

$$M_{\eta} = \sum_{\tilde{j}} \langle \eta | j \rangle \langle j | U | l \rangle \quad (10)$$

$$S_{\eta} = M_{\eta} \times N_{\eta} \quad (11)$$

The transmission coefficient can be represented as:

$$T = \sum_{\eta} \frac{M_{\eta} N_{\eta}}{z - \varepsilon_{\eta}} \quad (12)$$

Assuming that the interference effects between the different scattering channels can be neglected, the following equation is then obtained:

$$\begin{aligned} \bar{T} &= |T(E)|^2 = \sum_{\eta} |T(E)|_{\eta}^2 \\ &= \sum_{\eta} \frac{M_{\eta}^2 N_{\eta}^2}{(\varepsilon_{\eta} - E)^2 + \Gamma_{\eta}^2} \end{aligned} \quad (13)$$

$\Gamma_{\eta}$  is determined by the Fermi Golden rule:

$$\begin{aligned} \Gamma_{\eta} &= \pi \sum_{ij} \langle l | U | j \rangle \langle j | \eta \rangle^2 \sum_p \delta(E_f - E_p^S) + \\ &\pi \sum_{i'i} \langle l' | U | i \rangle \langle i | \eta \rangle^2 \sum_p \delta(E_f - E_p^D) \\ &= \pi \sum_{ij} \langle l | U | j \rangle \langle j | \eta \rangle^2 n^S(E_f) + \\ &\pi \sum_{i'i} \langle l' | U | i \rangle \langle i | \eta \rangle^2 n^D(E_f) \end{aligned} \quad (14)$$

where  $n^S(E_f)$  and  $n^D(E_f)$  are the densities of the states (DOS) of source and drain at the Fermi level  $E_f$ , respectively.

The Kubo formula is applied for calculating the current:

$$\begin{aligned} i_{SD} &= \sum_{\eta} \frac{emk_B T}{2\pi^2 \hbar^3} \int_{eV_D}^{\infty} dE |T(E)|_{\eta}^2 \times \\ &\left\{ \ln \left[ 1 + \exp \left( \frac{E_f + eV_D - E}{k_B T} \right) \right] - \right. \\ &\left. \ln \left[ 1 + \exp \left( \frac{E_f - E}{k_B T} \right) \right] \right\} \end{aligned} \quad (15)$$

where  $V_D$  is the applied bias,  $E_f$  is the Fermi energy of the electrode, and  $T$  is the temperature. The total current can be expressed as  $I_{SD} = Ai_{SD}$ , and  $A$  is the effective injection area of the metal surface. Assuming that each time an electron is injected, the effective injection area is  $A \approx \pi r_s^2$ , and here  $r_s = (3/4\pi n)^{1/3}$  is the average radius of an electron in metal and  $n$  is the density of the electron; the conductivity  $G$  is obtained as:

$$G = \partial I_{SD} / \partial V_D$$

The hybrid density functional theory (B3LYP / LANL2DZ) is used as given in the Gaussian 03 package<sup>[35]</sup> to optimize the geometries of the S-M-D supermolecules and to obtain the electronic structures of porphyrin and Cu-porphyrin. The two terminal hydrogen atoms are replaced by sulfur atoms, which can

form a chemical bond with Au of the electrode. The motion of electrons in the semi-infinite electrode is modeled by effective mass approximation.

## Results and Discussion

The transmission coefficient as a function of electron energy is shown in Fig. 2 for Au-CuPr-Au [ Fig. 2(A) ] and Au-Pr-Au [ Fig. 2(B) ]. The transmission peaks are close to 1.0 eV and 2.0 eV, which correspond to unoccupied molecular orbital levels, as indicated in eq. (13). The differences in transmission for Au-CuPr-Au and Au-Pr-Au are shown in Fig. 2.

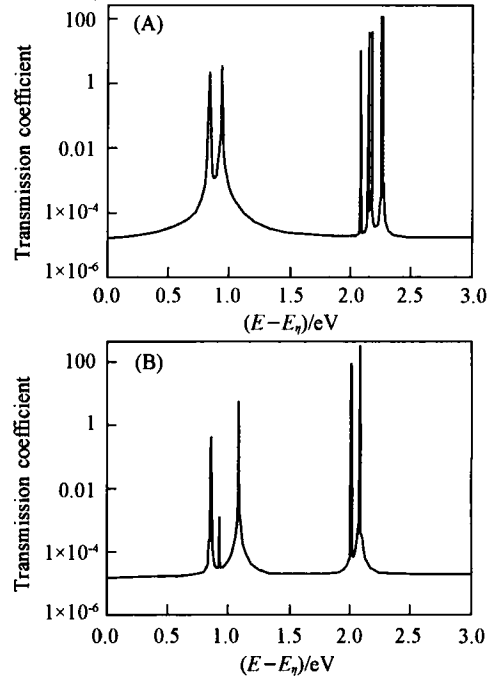


**Fig. 2** Transmission function of Au (3)-PrCu-Au (3) (A) and Au(3)-Pr-Au(3) (B) in the vicinity of the Fermi level

It must be noted that the numerator of eq. (13) is determined by the molecule-electrode coupling. In Tables 1 and 2, the contributions of each factor from the frontier orbital to the transmission is presented, for  $\alpha$ -spin electrons and  $\beta$ -spin electrons, respectively.

$S_{\eta}$  is basically the product of  $M_{\eta}$  as seen in eq. (11), which reflects the contribution of orbital  $\eta$  to the couplings with the left and right electrodes. The contributions were from the up and down spins sepa-

**Table 1** Contributions of  $\alpha$ -spin electrons of the frontier molecular orbitals to the electron transmission in molecular devices Au-CuPr-Au and Au-Pr-Au

$\eta$	$E_{\eta}$	CuPr				Pr				
		$10^4 S_{\eta}$	$10^3 M_{\eta}$	$10^3 N_{\eta}$	$10^2 \Gamma_{\eta}$	$E_{\eta}$	$10^4 S_{\eta}$	$10^3 M_{\eta}$	$10^3 N_{\eta}$	$10^2 \Gamma_{\eta}$
1	0.77	0.0365	0.060	60.80	5.670	0.85	0.451	68.300	0.660	6.8900
2	0.84	3.0100	53.000	5.67	4.070	0.87	0.564	67.100	0.841	6.6500
3	0.86	4.3100	48.900	8.81	3.540	0.94	0.115	0.190	60.700	5.8100
4	0.95	11.3000	22.100	51.30	4.170	1.09	3.460	5.790	59.800	4.9000
5	2.16	0.8140	8.680	9.38	0.115	2.01	0.351	5.990	5.850	0.0422
6	2.25	1.1200	9.710	11.50	0.742	2.08	2.380	14.100	16.900	0.9670

**Table 2 Contributions of  $\beta$ -spin electrons of the frontier molecular orbitals to the electron transmission in molecular devices Au-CuPr-Au and Au-Pr-Au**

$\eta$	$E_\eta$	CuPr				$E_\eta$	Pr			
		$10^4 S_\eta$	$10^3 M_\eta$	$10^3 N_\eta$	$10^2 \Gamma_\eta$		$10^4 S_\eta$	$10^3 M_\eta$	$10^3 N_\eta$	$10^2 \Gamma_\eta$
1	0.76	0.024	0.041	58.60	5.270	0.85	0.451	68.300	0.660	6.8900
2	0.84	4.530	52.000	8.71	3.750	0.87	0.564	67.100	0.841	6.6500
3	0.87	2.440	51.400	4.75	4.050	0.94	0.115	0.190	60.700	5.8100
4	0.95	10.900	20.800	52.40	4.240	1.09	3.460	5.790	59.800	4.9000
5	2.08	0.223	4.640	4.80	0.043	2.01	0.351	5.990	5.850	0.0422
6	2.18	0.708	8.080	8.76	0.100	2.08	2.380	14.100	16.900	0.9670

rately because of the presence of the copper atom; an unrestricted DFT scheme was applied.

The I—V characteristics for Au-CuPr-Au and Au-Pr-Au are given in Fig. 3.

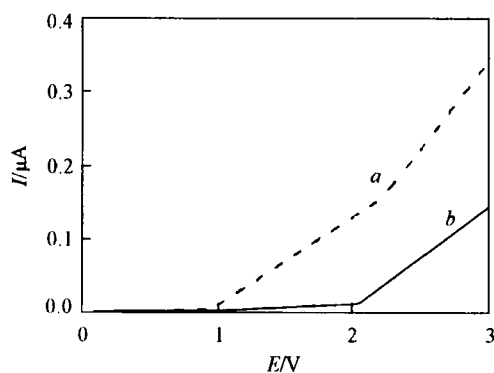


**Fig. 3 Comparison between the I—V characteristics of Au-CuPr-Au (a) and Au-Pr-Au (b)**

The conductance spectrum for Au-CuPr-Au and Au-Pr-Au are given in Fig. 4.

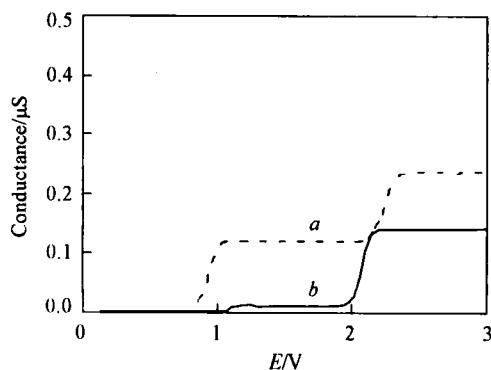


**Fig. 4 Comparison between the characteristic spectra of Au-CuPr-Au (a) and Au-Pr-Au (b)**

It can be seen that there is a threshold around 0.9 V and a further increase of current is observed at a bias of 2 V. It can be seen that the current increases more rapidly with the increase in bias voltage for the former device compared with the latter. This can be rationalized by the coupling of the molecular frontier orbitals with the electrodes. It can be seen from Tables 1 and 2 that factors  $S$  characterize the coupling between the molecules and the electrodes for the frontier orbitals and that for the second and the third unoccupied orbit-

als, factors  $S'$  are about  $3-4 \times 10^{-4}$  for CuPr, and these decrease to  $0.1-0.5 \times 10^{-4}$  for Pr. That is, the copper atom within the porphyrin effectively increases the coupling with the electrode.

The current is determined by the electrode's Fermi level, the Fermi distribution function, the transmission function, the external voltage, and the effective injection area of the metal surface. In this model, the two electrodes which are used are the Au electrodes. For the two molecular devices, there is no difference in the electrode's Fermi level, the Fermi distribution function, and the effective injection area of the metal surface.

According to equation (15), the current is determined by the transmission function, and the resonant transmission is attributed to the contribution of the molecular orbitals. As seen from Tables 1 and 2, the frontier orbitals for Au-CuPr-Au and Au-Pr-Au are grouped into two: the first part ranging from 0.76 to 0.95 eV; and the second part ranging from 2.08 to 2.27 eV, which are also clearly indicated in the transmission spectra (see the peaks in Fig. 2).

As mentioned above,  $S_\eta$  reflects the contributions of orbital  $\eta$ ,  $S_2$ ,  $S_3$ , and  $S_4$  in the first part because  $\alpha$  spin and  $\beta$  spin for Au-CuPr-Au are larger than those for Au-Pr-Au. However, in the second part, the  $S_\eta$  of Au-CuPr-Au is comparable to that of Au-Pr-Au for  $\alpha$  spin and  $\beta$  spin. The first group of orbitals for Au-CuPr-Au has a larger contribution compared with that for Au-Pr-Au; therefore, the conductance of the first step for Au-CuPr-Au is larger than that for Au-Pr-Au. However, from the first step to the second step, the variation in conductance is comparable for the two systems. That is, the conductances of the first steps of the two systems are 0.12  $\mu\text{S}$  and 0.01  $\mu\text{S}$ , respectively, for Au-CuPr-Au and Au-Pr-Au, whereas that of the second steps are 0.23  $\mu\text{S}$  and 0.14  $\mu\text{S}$ , respectively.

## Conclusions

The I—V characteristics of CuPr and Pr have been investigated by DFT coupled with the elastic scattering Green's function theory. It was found that CuPr

has better electron transport properties than Pr. This is attributed to the increased molecule-electrode overlap in the molecular frontier orbitals. From the analysis of the molecular frontier orbitals and the molecule-electrode coupling, the mechanism of electron transport and the contribution of metal atom in the organic molecule to the electron transport properties have been analyzed in detail.

## References

- [ 1 ] Joachim C. , Gimzewski J. K. , Aviram A. , *Nature*, **2000**, 408, 541
- [ 2 ] Nitzan A. , Ratner M. A. , *Science*, **2003**, 300, 1384
- [ 3 ] Reed M. A. , Zhou C. , Muller C. J. , *et al.*, *Science*, **1997**, 278, 252
- [ 4 ] Tans S. J. , Verschueren R. M. , Dekker C. , *Nature*, **1998**, 393, 49
- [ 5 ] Frank S. , Poncharal P. , Wang Z. L. , *et al.*, *Science*, **1998**, 280, 1744
- [ 6 ] Bumm L. A. , Arnold J. J. , Cygan M. T. , *et al.*, *Science*, **1996**, 271, 1705
- [ 7 ] Andres R. P. , Bielefeld J. O. , Henderson J. I. , *et al.*, *Science*, **1996**, 273, 1690
- [ 8 ] Chen J. , Reed M. A. , Rawlett A. M. , *et al.*, *Science*, **1999**, 286, 1550
- [ 9 ] Collier C. P. , Wong E. W. , Belohradsky M. , *et al.*, *Science*, **1999**, 285, 391
- [ 10 ] Gittins D. I. , Bethell D. , Schiffrin D. J. , *et al.*, *Nature*, **2000**, 408, 67
- [ 11 ] Donhauser Z. J. , Mantooth B. A. , Kelly K. F. , *et al.*, *Science*, **2001**, 292, 2303
- [ 12 ] Stokbro K. , Taylor J. , Brandbyge M. , *J. Am. Chem. Soc.*, **2003**, 125, 3674
- [ 13 ] Lang N. D. , Avouris P. , *Phys. Rev. B*, **2000**, 62, 7325
- [ 14 ] Reichert J. , Ochs R. , Beckmann D. , *et al.*, *Phys. Rev. Lett.*, **2002**, 88, 176804
- [ 15 ] Xu B. Q. , Tao N. J. , *Science*, **2003**, 301, 1221
- [ 16 ] Hu W. P. , Nakashima H. , Furukawa K. , *et al.*, *Appl. Phys. Lett.*, **2004**, 85, 115
- [ 17 ] Tans S. J. , Verschueren A. R. M. , Dekker C. , *Nature*, **1999**, 393, 49
- [ 18 ] Park H. , Park J. , Lim A. K. L. , *et al.*, *Nature*, **2000**, 407, 57
- [ 19 ] Mujica V. , Kemp M. , Ratner M. A. , *J. Chem. Phys.*, **1994**, 101, 6849
- [ 20 ] Tian W. , Datta S. , Hong S. , *et al.*, *J. Chem. Phys.*, **1998**, 109, 2847
- [ 21 ] Emberly E. G. , Kirzenow G. , *Phys. Rev. B*, **1998**, 58, 10911
- [ 22 ] Hall L. , Reimers J. R. , Hush N. S. , *et al.*, *J. Chem. Phys.*, **2000**, 112, 1510
- [ 23 ] Seminario J. M. , Zacarias A. G. , Tour J. M. , *J. Phys. Chem. A*, **1999**, 103, 7883
- [ 24 ] Wang C. K. , Fu Y. , Luo Y. , *Phys. Chem. Chem. Phys.*, **2001**, 3, 5017
- [ 25 ] Luo Y. , Wang C. K. , Fu Y. , *J. Chem. Phys.*, **2002**, 117, 10283
- [ 26 ] Lang N. D. , *Phys. Rev. B*, **1995**, 52, 5335
- [ 27 ] Ventra M. D. , Lang N. D. , *Phys. Rev. B*, **2001**, 65, 045402
- [ 28 ] Taylor J. , Guo H. , Wang J. , *Phys. Rev. B*, **2001**, 63, 245407
- [ 29 ] Brandbyge M. , Mozos J. L. , Ordejon P. , *et al.*, *Phys. Rev. B*, **2002**, 65, 165401
- [ 30 ] Ke S. H. , Baranger H. U. , Yang W. T. , *J. Am. Chem. Soc.*, **2004**, 126, 15897
- [ 31 ] Geng H. , Yin S. W. , Shuai Z. G. , *et al.*, *J. Phys. Chem. B*, **2005**, 109, 12304
- [ 32 ] Wang C. K. , Li H. H. , Li Y. D. , *et al.*, *Science in China, Series A*, **2002**, 32, 704
- [ 33 ] Taylor J. R. , *Scattering Theory*, Wiley, New York, **1972**
- [ 34 ] Economou E. N. , *Green's Functions in Quantum Physics*, Springer, Berlin, **1990**
- [ 35 ] Frisch M. J. , Trucks G. W. , Schlegel H. B. , *et al.*, *Gaussian 03*, Gaussian, Inc. , Pittsburgh PA, **2003**